Effects of Li$^+$ Doping Concentration on Structure and Photoluminescence of the Y$_2$O$_3$: Ho^{3+}/Yb^{3+} Up-conversion Film

Min Sun[1], Wenbo Hou[1], Juncheng Liu[1*] and Lifang Nie[1*]

[1]*School of Materials Science and Engineering, Tianjin Polytechnic University, Tianjin 300387, China.*

Authors' contributions

This work was carried out in collaboration among all authors. Authors MS and JL convinced and designed the methods and wrote the paper. Author WH completed most of the experimental work. Author LN analyzed the data. All authors read and approved the final manuscript.

Article Information

Original Research Article

ABSTRACT

The Li$^+$ co-doped Y$_2$O$_3$: Ho^{3+}/Yb^{3+} films were prepared with sol-gel method and spin-coating technique. The effects of Li$^+$ on the structure and luminescent properties of the films were investigated. The results show the grain size increased first and then decreased with the increase of Li$^+$ doping concentration. The crystal size of particles composing the film got the maximum value when Li$^+$ concentration took 4 mol%. As Li$^+$ doping concentration increased, the optical transmittance of the Y$_2$O$_3$: Ho^{3+}/Yb^{3+} film improved at first then reduced and got the maximum at 3 mol%. Excited with a 980-nm laser, there were two green emissions in the up-conversion emission spectra, one centered at 535 nm, the other at 550 nm, which ascribed to the $^5F_4 \rightarrow {}^5I_8$ and $^5S_2 \rightarrow {}^5I_8$ transitions of Ho^{3+}, respectively. The up-conversion luminescence intensity also increased firstly and then decreased with the Li$^+$ doping concentration increase, and got the highest value at 2 mol%.

Keywords: Photoluminescence; sol-gel; Y$_2$O$_3$ film; Ho^{3+}/Yb^{3+}; up-conversion.

_____

Corresponding author: E-mail: jchliu@tjpu.edu.cn, nielifang@tjpu.edu.cn;

1. INTRODUCTION

In recent years, the sustainable development of mankind is affected by the energy problem. The non-renewable resources were overused by a human being; the study about new energy has attracted wide attention. Solar cells have been industrialized and became a part of our lives. Most of the solar cells are based on crystalline silicon(Si), and it is found that the optimal efficiency of traditional single-junction silicon solar cells is 25% [1]. The transmission of sub-band-gap light is the major loss mechanism in Si solar cells. The infrared light accounted for more than 40% of the sunlight and can't be used. As a result, the use of the infrared light may directly affect the photoelectric conversion efficiency of solar cells. The research of up-conversion materials has developed quickly since Auzel discovered the up-conversion luminescence in 1960 [2,3]. Considering the feature of the up-conversion luminescence, it's a practical method to improve the photo-response of Si solar cells by preparing the up-conversion film on the surface of the Si solar cells.

It is well known that Y_2O_3 is an excellent host for the incorporation of lanthanide ions due to its unique properties such as high melting point (2439°C), high band gap energy (5.5 eV), high transparency in the 0.23-8 μm range and low phonon energy (600 cm^{-1}) [4,5]. Y_2O_3 upconversion materials doped with RE ions have been studied extensively [6-11]. It is well known that Ho^{3+}/Yb^{3+} is one of the most effective rare earth pairs. Yb^{3+} ion is a commonly used high-efficiency sensitizer. It can be pumped by 980-nm laser and transfer energy to Ho^{3+} ion [12,13]. The enhancement of luminescence in Ho^{3+}/Yb^{3+} system mainly depends on the highly efficient energy transfer (ET) from Yb^{3+} to Ho^{3+}. In recent years, more and more up-conversion materials have been studied based on Ho^{3+}/Yb^{3+} [14-16]. How to further improve the efficiency of upconversion luminescent films has been the goal of researchers. The ion doping is one of the effective ways. Li^+ doping has been used to improve the luminescence efficiency of Er^{3+}/Yb^{3+} luminescent films. Zou et al. doped Li^+ ions into TiO_2 nanocrystals by sol-gel method. The Li^+ ions promoted grain growth and increased crystallinity, which enhanced their luminescence intensity [17]. Mahalingam V et al enhanced the white light intensity by incorporating monovalent Li^+ ions into the $GdVO_4$ matrix [18].

Herein, Li^+ doping will be used to improve the luminescence efficiency of Y_2O_3: Ho^{3+}/Yb^{3+} thin luminescent films prepared with the sol-gel method and spin-coating technique. The effects of Li^+ on the structure and photoluminescence characteristics of Y_2O_3: Ho^{3+}/Yb^{3+} thin films will be investigated.

2. EXPERIMENTS

2.1 Preparation of Sol

All the starting chemical reagents in this experiment come from regular manufacturers without further treatment. Yttrium oxide [Y_2O_3] (99.99%), was from Guangdong Wengjiang Reagent Co., Ltd. Ytterbium nitrate [$Yb(NO_3)_3 \cdot 5H_2O$], Holmium nitrate [$Ho(NO_3)_3 \cdot 5H_2O$], Lithium nitrate [$LiNO_3 \cdot H_2O$] (98.5%) and citric acid [$C_6H_8O_7 \cdot H_2O$] (99.5%) were from Tianjin Fengchuan Chemical Reagent Technology Co., Ltd. Nitric acid [HNO_3] (66%-68%) was from Xinsheng Chemical Co., Ltd.

The concentration of Li^+ is the only variable. The concrete Li^+ dosage in this experiment is shown in Table 1. Firstly, the above-mentioned chemicals were added to the suitable amount of nitric acid solution, heated and stirred until they were dissolved fully. Then a certain amount of citric acid solution was added to the solutions and stirred at 80°C for 30 min. Finally all the solutions were placed in a water bath at 90°C to react further to form a sol.

Table 1. The specific chemical compositions with different Li^+ concentration

Li^+ concentration	Chemical compositions
0 mol%	Y_2O_3+ $Yb(NO_3)_3 \cdot 5H_2O$+ $Ho(NO_3)_3 \cdot 5H_2O$
1 mol%	Y_2O_3+ $Yb(NO_3)_3 \cdot 5H_2O$ + $Ho(NO_3)_3 \cdot 5H_2O$+$LiNO_3 \cdot H_2O$
2 mol%	Y_2O_3+ $Yb(NO_3)_3 \cdot 5H_2O$ + $Ho(NO_3)_3 \cdot 5H_2O$ +$LiNO_3 \cdot H_2O$
3 mol%	Y_2O_3+ $Yb(NO_3)_3 \cdot 5H_2O$ + $Ho(NO_3)_3 \cdot 5H_2O$ +$LiNO_3 \cdot H_2O$
4 mol%	Y_2O_3+ $Yb(NO_3)_3 \cdot 5H_2O$ + $Ho(NO_3)_3 \cdot 5H_2O$ +$LiNO_3 \cdot H_2O$
5 mol%	Y_2O_3+ $Yb(NO_3)_3 \cdot 5H_2O$ + $Ho(NO_3)_3 \cdot 5H_2O$ +$LiNO_3 \cdot H_2O$

2.2 Preparation of Films

The quartz glass with a size of 50 mm × 50 mm was chosen as a substrate. Firstly, all the substrates were cleaned by ethanol, then cleaned ultrasonically for 20 min to remove the stubborn stains. Next, they were cleaned with acid and alkali liquids for 30 minutes. Then they were washed with deionized water and were dried in oven at 80°C. The ready sol above was deposited on the substrates to form thin films with spin-coating. After deposition, the samples were dried at 200°C in an oven for 30 min followed annealing at 550°C for 2 h.

2.3 Characterization

The surface morphology of the film was observed with field emission scanning electron microscopy (FE-SEM, Hitachi S-4800). The crystal structure of Y_2O_3 was characterized by X-ray diffraction (XRD, D8 DISCOVER, BRUKERAXS, Germany). The transmittance of the film within the visible and near-infrared wavelength was tested with UV-3600 spectrophotometer. The photoluminescence (PL) spectrum was recorded with Hitachi F-4500 fluorescence spectrophotometer pumped at 980-nm laser.

3. RESULTS AND DISCUSSION

3.1 Surface Morphology and Crystal Structure of the Film

The surface morphology of the film is shown in Fig. 1. As the surface morphology of Y_2O_3 thin films is very similar, taking the doping concentration of 2 mol% and 5 mol% as examples, it can be seen that the surface of Y_2O_3 thin films is very compact and composed of fine and round grains. The doping of Li^+ has little effect on the surface morphology of the films. However, it may affect its crystallinity and grain size, so we also analyzed the crystal structure of the sample.

Fig. 2 shows the XRD patterns of the samples with different Li^+ concentrations. As shown in Fig. 2(a), all the diffraction peaks can be well consistent with the cubic phase of Y_2O_3 (JPCDS 65-3178). No any excessive peaks are detected, which indicate that there are no new crystalline phases and other impurities in the sample. Li^+ ion and Yb^{3+}/Ho^{3+} rare earth ions have been successfully doped into the Y_2O_3 lattice, and the doping did not change the lattice structure of the matrix. In addition, with the increase of Li^+ concentration, the main diffraction peaks become stronger and sharper before the concentration of Li^+ reaches 5 mol%. This phenomenon indicates that Li^+ doping is beneficial for Y_2O_3 to form a high crystallization.

In addition, it can be found that the position of the main diffraction peak, (222) crystal plane peak, shifts a little after Li^+ ions doping. Fig. 2 (b), a local magnification graph, shows this shift more clearly. Before the doping concentration of Li^+ increases to 2 mol%, all peaks move slightly to the right with the increase of Li^+ doping concentration. While Li^+ increases to 4 mol%, all peaks move in the opposite direction and then shift to the right again from 4 mol% to 5 mol%.
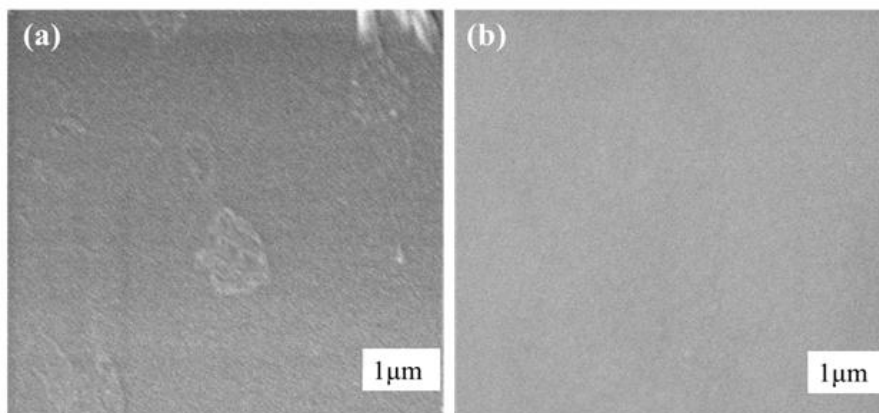

Fig. 1. The surface morphology of the Y_2O_3: Ho^{3+}/Yb^{3+} film with different Li^+ concentration (a) 2 mol% Li^+; (b) 5 mol% Li^+

The position of the diffraction peak and the average grain size, as shown in Table 2, the average grain size of the samples were calculated according to the Debye-Scherrer formula: $D = K\lambda/\beta cos\theta$.

The radius of Li^+ (0.76Å) is less than Y^{3+}(0.90Å). According to the Bragg's Law: $2d sin\theta = n\lambda$ (d is the crystalline interplanar spacing, θ is the angle between X-ray and crystal planes; n is the diffraction series, λ is the incident wavelength of X-ray, 0.154 nm). When the Li^+ ion replaces Y^{3+}, the interplanar spacing is smaller, resulting in a larger diffraction angle θ, and the diffraction peak shifts to a higher angle. However, when Li^+ ion enters the lattice gap position, the interplanar spacing is increased, the diffraction angle θ is decreased. According to the variation of the main diffraction peak in Table 2, when the doping concentration of Li^+ is less than 2 mol%, Li^+ ions replace Y^{3+} ions, so that the diffraction peak shifts to the right; when the Li^+ concentration is more than 2 mol%, the extra Li^+ ions enter the gap position of the Y_2O_3 lattice, therefore the diffraction peak shifts to the left. Finally, when the Li^+ doping concentration reaches 5 mol%, more Li^+ ions replace the Y^{3+} ions, and the diffraction peak shifts to the right again. Compared with the undoped sample, the average grain size of Li^+ doped samples increases with the increase of Li^+ doping concentration, which indicates that the

incorporation of Li^+ ions significantly improves the crystallinity and increases the grain size of the film.

3.2 Transmittance of the Film

Fig. 3 shows the transmittance curves of Li^+ doped Y_2O_3: Ho^{3+}/Yb^{3+} in the visible-infrared region. As can be seen from Fig. 3, all the films have rather a high transmittance in the whole spectrum range, the lowest value at about 880 nm is also more than 83%. The transmittance in the visible region (380-780 nm) is higher than that in the near infrared region (780-1300 nm). With the increase of Li^+ doping concentration, the transmittance of the films increases first and then decreases. When the concentration of Li^+ is 3 mol%, the transmittance of the film is the highest, while that of the film without Li^+ is the lowest. The transmittance of each sample shows a similar trend with the change of wavelength. With the increase of wavelength, the transmittance of the films increases sharply in the range of 350-400 nm, then decreases in the range of 400-440 nm, increases again in the range of 440-535 nm, then decreases, and finally increases slowly after 1000 nm. The transmittance reaches its maximum in the ultraviolet region. The fluctuation at 850 nm is caused by the light source switching of the test instrument itself, and this fluctuation occurs in all curves.
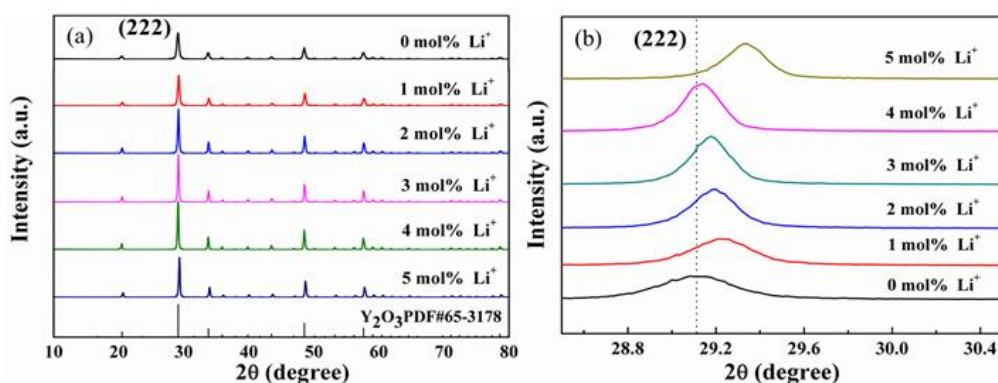

Fig. 2. (a) Effect of Li^+ ion on the XRD patterns of Y_2O_3: Ho^{3+}/Yb^{3+} samples; (b) the shift of the main diffraction peaks (222) of the XRD patterns

Table 2. The grain size of the samples with different Li^+ concentrate

Li^+ concentration	0 mol%	1 mol%	2 mol%	3 mol%	4 mol%	5 mol%
2θ	29.12	29.26	29.20	29.18	29.14	29.34
Average grain size	23 nm	30 nm	42 nm	47 nm	54 nm	43 nm
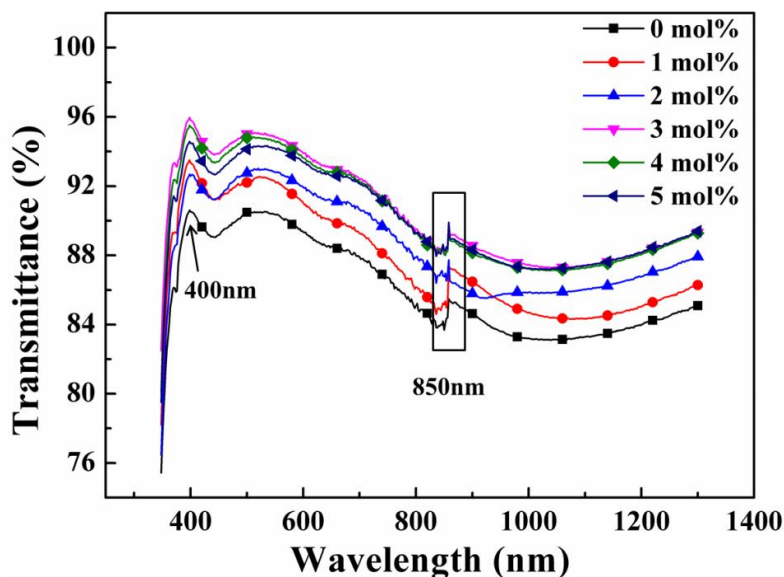
Fig. 3. Effect of the Li$^+$ concentration on the transmittance of Y_2O_3: Ho^{3+}/Yb^{3+} films

3.3 Up-conversion Luminescence of the Film

Fig. 4(a) shows the up-conversion emission spectra of Y_2O_3: Ho^{3+}/Yb^{3+} films under 980-nm excitation. It is obvious from Fig. 4(a) that all the film samples have two green emissions. According to the energy levels structure of Ho^{3+} and the previous work [19], the strong green emission at 535 nm is ascribed to the $^5F_4 \rightarrow ^5I_8$ transition of Ho^{3+}. The other one at 550 nm is assigned to the $^5S_2 \rightarrow ^5I_8$ transition of Ho^{3+}. It can be seen that the luminescence intensity of the undoped Li$^+$ ion sample is much weaker than that of other samples.

In order to study the variation of the emission peaks intensity, Fig. 4(b) shows the curves of the two green emission peaks' intensity with the concentration of Li$^+$ ions. The intensity of both green emissions increases first and then decreases. When the doping concentration of Li$^+$ ions increases from 0 mol% to 2 mol%, the emission intensity increases. Then the emission intensity decreases as the Li$^+$ doping concentration continues to increase. That is to say, the up-conversion luminescence intensity reaches the maximum value at 2 mol% concentration.

For 535 nm green light emission, the luminescence intensity of the sample doped with 2 mol% Li$^+$ ions is twice as strong as that of the undoped sample, while the green emission at

550 nm is 9.2 times that of the undoped sample. These phenomena indicate that up-conversion luminescence intensity of the RE-doped Y_2O_3 thin films can be effectively enhanced by Li$^+$ doping, which can be explained that Li$^+$ promotes 4f electron transition. Because whether Li$^+$ ions enter the lattice gap or replace RE^{3+} ions, it can reduce the crystal field symmetry and improve the luminescence intensity. Moreover, with the increase of Li$^+$ concentration, the change of green emission at 550 nm is different. When the concentration of Li$^+$ is less than 2 mol%, the intensity of the green emission at 550 nm is very low. However, when the Li$^+$ doping concentration increase to 2 mol%, the luminescence intensity at 550 nm increases more than that at 535 nm, which suggests that more Li$^+$ can improve non-radiative transition probability of $^5S_2 \rightarrow ^5I_8$ to a greater extent.

In order to further clarify the mechanism of Li$^+$ doping to enhance luminescence intensity, we observed the upconversion luminescence intensity of Y_2O_3: Ho^{3+}/Yb^{3+} doped with 2 mol% Li$^+$ as a function of pump power and analyzed it. The excitation wavelength is 980 nm, as shown in Fig. 5. The upconversion intensity I is proportional to the P^n, which can be expressed as $\ln I = n \ln P + A$, where A is a constant, P is the pump power of the laser, and n is the number of photons required to achieve green upconversion emission. Namely, the slope of the fitted curve is the number of photons processed by the double logarithm of light intensity and pump power. As

can be seen from Fig. 5, the slopes of the fitted curves for the green emissions at 535 nm and 550 nm are 1.84 and 1.80, respectively. This indicates that the green emissions of Li$^+$ doped Y_2O_3: Ho^{3+}/Yb^{3+} thin film are a two-photon process.

Fig. 6 schematically shows the energy transfer mechanism of Ho^{3+}-Yb^{3+} system. It can be seen from Fig. 6 that the energy of anti-stokes transition in 4f-4f of Ho^{3+} ion comes from the high sensitization of Yb^{3+} ion. Moreover, from the conclusion of the previous section, green light emission is a two-photon process. The basic process is as follows: Yb^{3+} ions first absorb 980-nm excitation light from the pumped laser, then transition from ground state level $^2F_{7/2}$ to $^2F_{5/2}$

and transfer its energy to neighbouring Ho^{3+} ions. There may be three energy transfer modes from Yb^{3+} to Ho^{3+} ions. Firstly, Ho^{3+} ion accepts energy from $^2F_{5/2}$ level of Yb^{3+} ion and transits from ground state $^5I_8$ to $^5I_6$, which is the ET1 process: $^2F_{5/2}(Yb^{3+})$ + $^5I_8(Ho^{3+})$ → $^2F_{5/2}(Yb^{3+})$ + $^5I_6(Ho^{3+})$. Then, Ho^{3+} ions at $^5I_6$ level continue to receive energy from Yb^{3+}, through the processes of ET2: $^2F_{5/2}(Yb^{3+})$ + $^5I_6$ (Ho^{3+}) → $^2F_{7/2}(Yb^{3+})$ + $^5F_4(Ho^{3+})$ and ET3: $^2F_{5/2}(Yb^{3+})$ + $^5I_6(Ho^{3+})$ → $^2F_{7/2}(Yb^{3+})$ + $^5S_2(Ho^{3+})$, so that the excited Ho^{3+} ions accumulated at $^5F_4$ and $^5S_2$ levels. Finally, the 535 nm green emission is obtained through the radiative transition from $^5F_4$ to $^5I_8$ level. The green emission centred at 550 nm is related to the $^5S_2 \rightarrow ^5I_8$ transition.
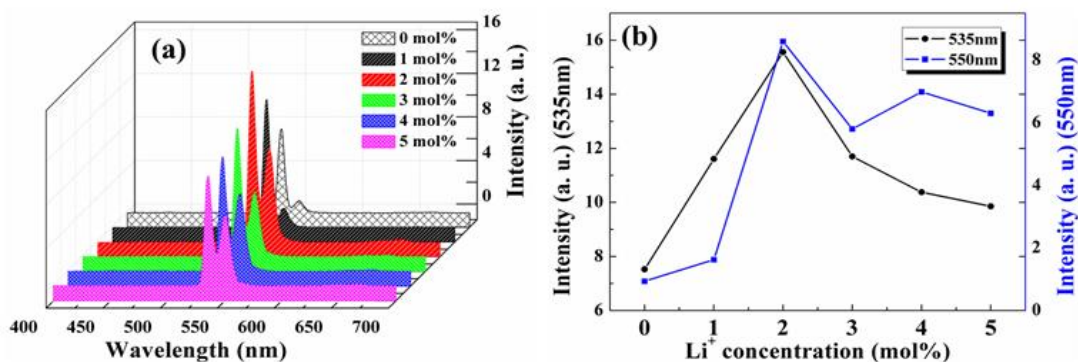

Fig. 4. (a) Effect of the Li$^+$ concentration on the up-conversion spectra of Y_2O_3: Ho^{3+}/Yb^{3+} films; (b) The main peaks change at 535 nm and 550 nm
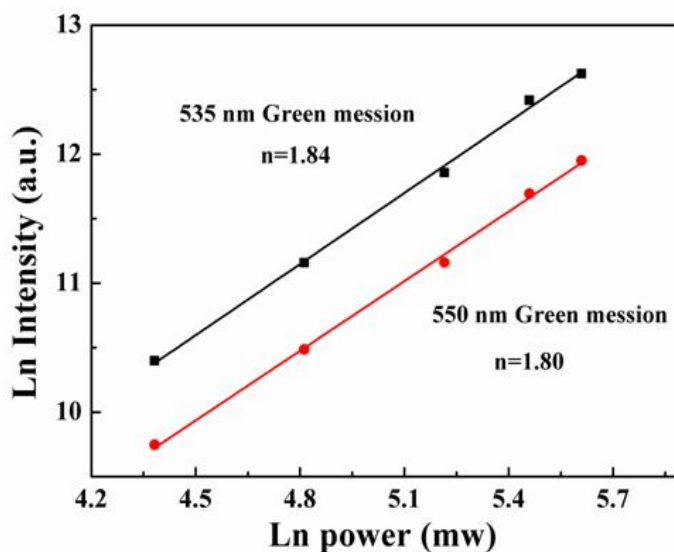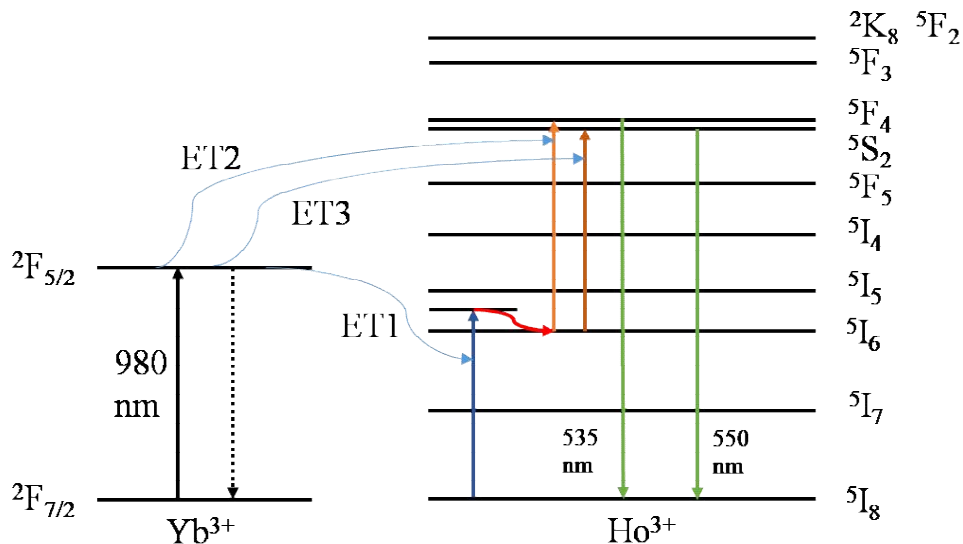

Fig. 5. Dependence of the upconversion luminescence intensity on excitation power forY_2O_3: Ho^{3+}/Yb^{3+} film with Li$^+$ 2 mol%

Fig. 6. Energy level diagram of Yb^{3+}-Ho^{3+} co-doped Y_2O_3 film as well as the probable up-conversion mechanisms

The main reason why Li^+ ions doping can enhance luminescence intensity is as follows: First, the appropriate Li^+ ions doping improves the crystallinity of the sample, which is beneficial to increase the number of luminescent centres. In addition, the substitution and filling of Li^+ ions reduce the local symmetry of the crystal field, so that break the parity forbidden of Ho^{3+} and Yb^{3+} ions, increase the probability of radiation transition. These can promote the luminescence process.

4. CONCLUSIONS

In summary, Y_2O_3: Ho^{3+}/Yb^{3+} films were prepared with sol-gel method and spin-coating technique. The effects of Li^+ concentration on the structure and the photoluminescence of the Y_2O_3: Ho^{3+}/Yb^{3+} up-conversion film were investigated. It is found that when the Li^+ concentration is 4 mol%, the crystal particle size is the largest, which indicates that it is a feasible method to accelerate crystal growth by doping Li^+. It is beneficial to improve the crystallinity of Y_2O_3. The transmittance of the Y_2O_3: Ho^{3+}/Yb^{3+} films improves first and then decreases gradually, and gain the highest value when the concentration is 3 mol%.

When the film pumped with a 980-nm laser, the UC emissions centred at 535 nm and 550 nm wavelengths are observed, corresponding to $^5F_4\rightarrow{}^5I_8$ and $^5S_2\rightarrow{}^5I_8$ transitions of Ho^{3+} ions, respectively. In addition, with the increase of Li^+ doping concentration, the film's up-conversion luminescence intensity increases at first and then decreases, and reaches its maximum when Li^+ concentration is 2 mol%.

COMPETING INTERESTS

Authors have declared that no competing interests exist.

REFERENCES

1. Martin A. Green. The Path to 25% Silicon Solar Cell Efficiency: History of Silicon Cell Evolution. Progress in Photovoltaics Research & Applications. 2010;17(3):183-189.
2. Auzel F, Acad CR. Sci. Paris. 1966; 263B:819.
3. Auzel F, Acad CR. Sci. Paris 1966;262: 1016.
4. Zhu JQ, Zhu YK, Shen WX, Wang YJ, Han JC, Tian G, et al. Growth and characterization of yttrium oxide films by reactive magnetron sputtering. Thin Solid Films. 2011;519(15):4894-4898.
5. Chen GY, Liu Y, Zhang YG, Somesfalean G, Zhang ZG, Sun Q, et al. Bright white upconversion luminescence in rare-earth-ion-doped Y_2O_3 nanocrystals. Applied Physics Letters. 2007;91:133103.
6. Ali AG, Dejene BF, Swart HC. Temperature dependence of structural and

luminescence properties of Eu^{3+}-doped Y_2O_3 red-emitting phosphor thin films by pulsed laser deposition. Applied Physics A. 2016;122(382):1-9.

7. Kaur M, Eisen DP, Brahme N, Singh P, Sahu IP. Photoluminescence properties of rare-earth-doped (Er^{3+}, Yb^{3+}) Y_2O_3 nanophosphors by a combustion synthesis method. Luminescence. 2016;31(3):728-737.

8. Meng FL, Luo Y, Zhou YL, Zhang JW, Zheng YZ, Cao GZ, et al. Integrated plasmonic and upconversion starlike Y_2O_3: Er/Au@TiO_2 composite for enhanced photon harvesting in dye-sensitized solar cells. Journal of Power Sources. 2016; 316:207-214.

9. Qiao YM, Guo H. Upconversion properties of Y_2O_3: Er films prepared by sol-gel method. Journal of Rare Earths. 2009; 27(3):406-410.

10. Dikovska AOg, Atanasov PA, Dimitrov IG, Vasilev C, Kocourek T, Jelinek M. Structural and optical properties of Er, Yb co-doped Y_2O_3 thin films. Applied Surface Science. 2006;252(13):4569-4572.

11. Lian J, Yang L, Chen XY, Liu GK, Wang LM, Ewing RC, et al. Deposition of ultrathin rare-earth doped Y_2O_3 phosphor films on alumina nanoparticles. Nanotechnology. 2006;17(5):1351-1354.

12. Martı́n IR, Ve´lez P, Rodrı́guez VD, Rodrı́guez-Mendoza UR, Lavı́n V. Upconversion dynamics in Er^{3+} dopped fluoroindate glasses. 1999;55:935-940.

13. Boyer JC, Vetrone F, Capobianco JA, Speghini A, Bettinelli M. Yb^{3+} ion as a sensitizer for the upconversion luminescence in nanocrystalline $Gd_3Ga_5O_{12}$: Ho^{3+}. Chemical Physics Letters. 2004;390(4):403-407.

14. Cai MZ, Zhou BE, Tian Y, Zhou JJ, Xu SQ, Zhang JJ. Broadband mid-infrared 2.8 μm emission in Ho^{3+}/Yb^{3+}-codoped germanate glasses. Journal of Luminescence. 2016; 171:143-148.

15. Hu YB, Dou RJ, Qiu JB. Spectroscopic properties and energy transfers in Tb^{3+}/Ho^{3+}/Yb^{3+} tri-doped oxyfluoride silicate glasses. Journal of Non-Crystalline Solids. 2015;420:12-16.

16. Peng SX, Wu LB, Wang B, Yang FJ, Qi YW, Zhou YX. Intense visible upconversion and energy transfer in Ho^{3+}/Yb^{3+} codoped tellurite glasses for potential fiber laser. Optical Fiber Technology. 2015;22:95-101.

17. Zou KS, Dong GZ, Liu JC, Xu BX, Wang DP. Effects of calcination temperature and Li^+ ions doping on structure and upconversion luminescence properties of TiO_2: Ho^{3+}-Yb^{3+} nanocrystals. Journal of Materials Science & Technology; 2018.

18. Venkataramanan M, Rafik N, Fiorenzo V, John AC. Enhancing upconverted white light in Tm^{3+}/Yb^{3+}/Ho^{3+}-doped $GdVO_4$ nanocrystals via incorporation of Li^+ ions. Optics Express. 2012;20(1):111-119.

19. Ledemi Y, Manzani D, Ribeiro SJL, Messaddeq Y. Multicolor up conversion emission and color tunability in Yb^{3+}/Tm^{3+}/Ho^{3+} triply doped heavy metal oxide glasses. Optical Materials. 2011; 33(12):1916-1920.